JOURNAL OF MATERIALS SCIENCE 30 (1995) 6303–6308

X-ray fluorescence study of fine powders of wolframite ores with SiO_2 and WO_3 major phases

S. C. SRIVASTAVA, A. N. DAS, L. P. PANDEY
Analytical Chemistry Division, National Metallurgical Laboratory, Jamshedpur 831 007, India
S. RAM
Institut für Metallforschung, Technische Universität Berlin, D-10623, Berlin, Germany

Single phase pure SiO_2 exhibits a strong and symmetric X-ray fluorescence (XRF) peak at 1.741 keV, which does not depend much on the size of the particles. Moreover, the separated particles of 30–110 μm size strongly interact with 5–20 wt % WO_3 additions of similar particle sizes, and show dramatic changes of peak intensity (I_p), half-bandwidth $2\Delta\theta_{1/2}$, (i.e. the full width at the half peak-intensity), and integrated intensity (I) of the signal as a function of size of the particles. The WO_3 fluoresces at the relatively higher energy of 8.39 keV with adversely modified intensity I_p or I in such a peculiar way that the total intensity I_t in the two signals of the two WO_3 and SiO_2 phases is nearly constant. The results are tested and applied to XRF analyses of a wolframite ore having SiO_2 and WO_3 as the two major phases. In all these examples, the intensities of the SiO_2 and WO_3 signals vary, basically due to the expected macroscopic electromagnetic interactions between the two phases.

1. Introduction

X-ray fluorescence (XRF) usually measures the intensity of the fluorescence radiation emitted from a substance in excitation of a core level electron. It is a purely non-destructive technique used to measure the desired specimen without disturbing its structure during the sampling process. Obviously, it is a very reliable method for unambiguously analysing the effects of impurities, defects or other local structures on fluorescence of a particular phase in a pure or mixed material.

According to Berry *et al.* [1], the XRF intensity depends considerably on

1. compaction of the sample,
2. back scattered radiation, or
3. presence of secondary phase, if any.

Here, particle size of the specimen apparently influences the first two factors. In this case, we expect a minor variation in XRF intensity as a function of the particle size of the specimen. Claisse and Samson [2] and Bernstein [3] argue that the small sized particles provide a large specific surface to exhibit a reasonably manifested fluorescence on smaller and smaller particles. Note that the fluorescence is not a surface limited process. It accounts for the excitation of electrons of individual atoms in a specimen of micron order thickness according to wavelength λ of the incident (excitation) radiation and the absorption coefficient of the associated species.

Of course, the electronic and atomic structures (which are principal sources of any electron induced radiation) of the system are modified with sufficiently fine particles. As a result, for example, nanocrystals have a solely different electronic structure than regular crystals, as demonstrated essentially by different electronic, magnetic and other physical properties as described in [4]. This investigation is therefore undertaken to demonstrate these observations using XRF of pure and binary mixtures of SiO_2 with WO_3 or wolframite ores. The results can be utilized to understand XRF of minerals, ores and other materials, particularly to obtain their accurate chemical analyses.

2. Experimental details

Pure (99.9%) SiO_2 of varying particle sizes, in the range 0.01–110 μm, were crystallized by annealing different batches of a silica glass at different temperatures, in the range 500–800 °C, for about 30 min [5–7]. WO_3 is commercially available and it was used as received. The wolframite ores were collected from Bankura mines (India) and were carefully washed and rinsed in dilute H_2SO_4 to remove any dust and other impurities. The sample was crushed and powdered, with particle sizes in the range 30–110 μm, using a ball milling. The powders of five representative particle sizes, namely 106, 75, 63, 53 and 44 μm, were separated by sieving with five different sieves of aforesaid sizes. Their chemical compositions were determined independently by chemical analyses. The results along with the specific gravities, which were measured by a gas displacement technique in a penta-pycnometer, are given in Table I.

XRF of the various samples were studied in powder and/or pellet forms. The pellets of 38 mm diameter

0022–2461

TABLE I Chemical composition, particle size and specific gravity of the wolframite ores used in the present XRF studies

Sample	Percentage (wt %) SiO_2	WO_3	Particle size (μm)	Specific gravity
A	24.0	8.2	106	3.40
B	23.6	8.8	75	3.45
C	23.8	9.5	63	3.57
D	20.6	10.2	53	3.65
E	19.7	13.0	44	3.75

were achieved by compressing the powders with boric acid (used as a backing material) by a hydraulic press using usually at three different pressures of 5, 10 and 20 tons cm^{-2} [8, 9].

An automatic wavelength dispersive X-ray spectrometer (Philips, model PW-1404/10), with a Cr–Au dual anode and the diffracting media of LiF (2 0 0) and PET (0 0 2) crystals of interplanar spacings $d = 0.2004$ and 0.437 nm, respectively, was used to record the XRF spectra over a 2θ° scale. Other experimental parameters, including the wavelength of the radiation used to excite the specimen to monitor the desired XRF spectrum programmed through a computer, are summarized in Table II.

3. Results and discussion

Fig. 1 shows XRF spectra of pure SiO_2 of two different particle sizes, i.e. 0.01 and 106 μm. A prominent band, intrinsic to the SiK_α transition, appears at 1.741 keV or 2θ angle of about 109° in either sample. There is no appreciable change in shape as well as size of the signal with change of particle size. Another signal, which appears at 107.8° and which is relatively much weaker, is due to the SiK_β transition, as discussed in detail elsewhere [1, 2].

The intensity of the fluorescence of SiO_2 is very sensitively diminished, by as much as a factor of 6, on adding a secondary phase of 10 wt % WO_3 (Fig. 2). To analyse whether the WO_3 additive influences both the bands of SiO_2 in the same fashion, we recorded several spectra at different I^n versus 2θ scales. The I^n versus 2θ spectra with smaller powers of n than 1 provide reasonably better resolved intensity in the weak band at 107.8°. As a consequence, a typical $I^{1/2}$ versus 2θ spectrum, shown in Fig. 2b, demonstrates an adequately magnified relative intensity in this particular band in curve (3) or curve (4) measured for the pure or mixed SiO_2 with 10 w t % WO_3. It eventually allowed comparison of the relative intensities in the two bands, which, of course, have been found to be apparently equally affected by WO_3 additions to the SiO_2 powders.

The nearest (WL_α) energy level at 8.39 keV of WO_3 is far away from the SiK_α energy level at 1.74 keV (or $2\theta = 109°$) of SiO_2 and hence there is no chance of mixing the two energy levels by the resonance. Consistently, the SiK_α band of SiO_2 always appeared at the same position of $2\theta = 109°$ in Figs 1 and 2 irrespective of admixed WO_3 powders. To get further details about the interaction, if any, between SiK_α and WL_α energy levels, we systematically studied wolframite ores which contained mainly SiO_2 and WO_3 (for exact compositions see Table I). Different specimens from the same batch of the ore were prepared by milling them for different periods of time. It yielded finely divided powders of different particle sizes, ranging from 30 to 110 μm, which were separated by sieving with different mesh sized sieves. In fact, to separate a specific powder of strictly homogeneous particle size is not easy using this technique and the particle sizes listed in Table I represent the average values of about 50% particles of the reported value.

Heterogeneity in the particle size, especially in the case of the ores, where different particles often bear different compositions, is a very important parameter which apparently sensitively influences the XRF intensity distribution. In the present example, the WO_3 is a characteristically very hard material compared to the SiO_2 and it leads to modified compositions of the resulting powders separated by milling and sieving. The SiO_2, which intimately adheres WO_3, is ground faster and readily comes out in the powders of relatively small sized particles. Hence, to compare the relative intensities in XRF of these powders, we measured their chemical compositions separately, as mentioned in the experimental section, and normalized the XRF intensity scale per unit concentration of associated species in the specimen.

Fig. 3, compares XRF of SiO_2 in SiK_α transition in five representative powders, A, B, C, D and E of the wolframite ore with particle sizes 106, 75, 63, 53 and 44 μm, respectively. The normalized intensity I per unit concentration of SiO_2 in the respective powders regularly decreased with decreasing particle size in

TABLE II Experimental conditions used to measure the XRF of the present samples

Parameters	Fluorescence W	Si
Fluorescent radiation	L_α (0.1476 nm)	K_α (0.7126 nm)
Power of the source	60 kV/50 mA	45 kV/65 mA
Dispersing media	LiF (2 0 0) ($2d = 0.4008$ nm)	PET (0 0 2) ($2d = 0.8742$ nm)
Optical path	Vacuum (2 Pa)	Vacuum (2 Pa)
Diffraction angle, 2θ	43°	109.01°
Detector	Flow proportional + Scintillation Counter	Flow proportional + Scintillation Counter
Collimator	Fine	Coarse

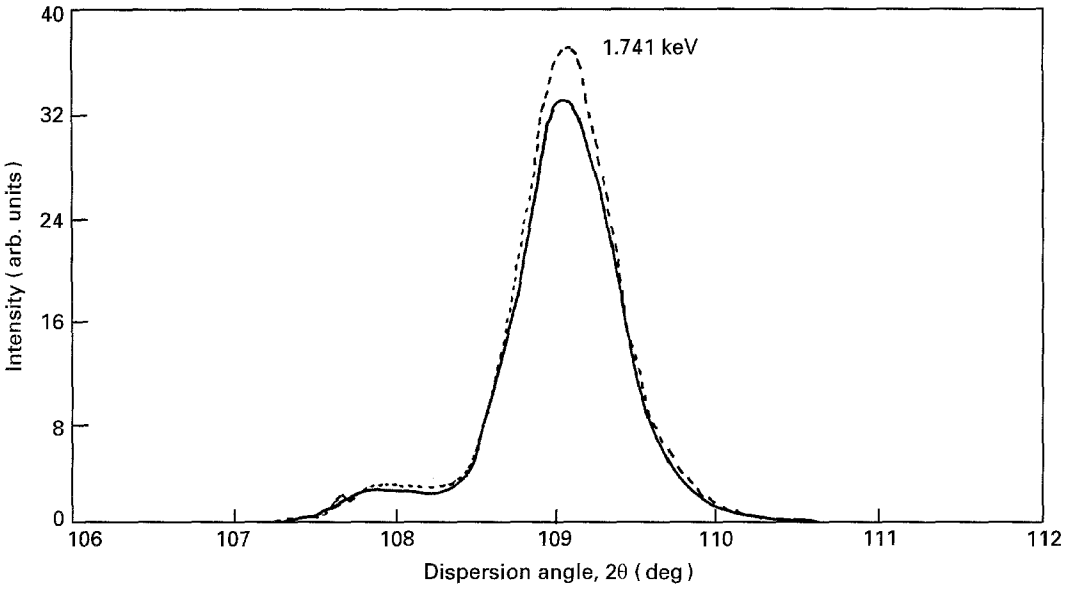

Figure 1 XRF of nanocrystalline (– – –) and well-crystallized (——) SiO_2 powders.

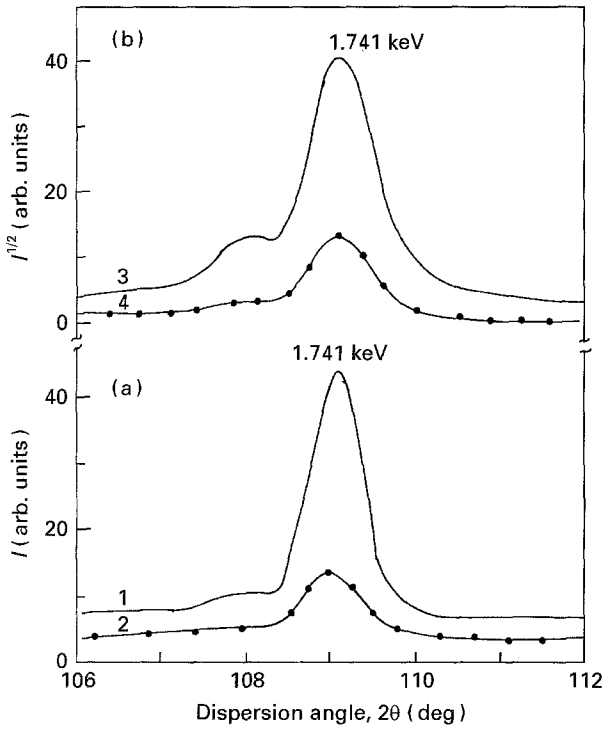

Figure 2 XRF of pure (curves 1 and 3) and mixed (curves 2 and 4) SiO_2 with 10 wt % WO_3 recorded in (a) normal and (b) square-root of intensity (I) scales. The scales given on Y-axis apply to curves 1 and 3. These are to be multiplied by a factor of 0.25 in curve 2 and by 0.50 in curve 4.

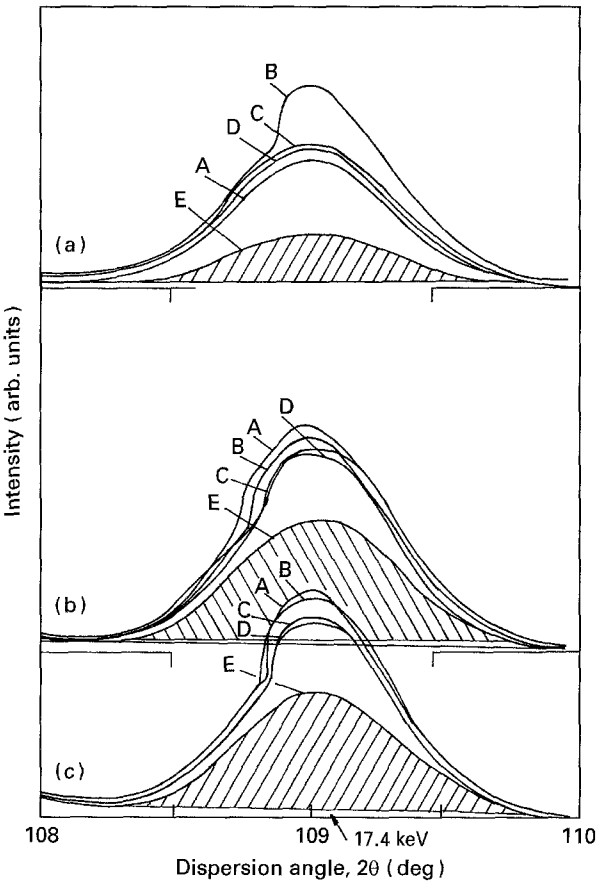

Figure 3 XRF of SiO_2 in the wolframite ore of different particle sizes of 106, 75, 63, 53 and 44 μm in A, B, C, D and E, respectively; (a) as-received powders, and those pelletized at (b) 10 tons cm^{-2} and (c) 20 tons cm^{-2} applied pressures.

powders B, C, D and E. The present observation is contrary to that reported by Claisse and Samson [2] that small particles usually provide large surfaces to exhibit reasonably manifested fluorescence on the fine particle powders. Here, sample A, which had reasonably big particles of about 106 μm, apparently did not obey the trend shown by the other samples, B to E, due to a lack of homogeneous distribution of the involved phases. Actually, the big particles contained both SiO_2 and WO_3 very intimately adhering together. They did not allow uniform exposure to the individual components in order to measure their correct XRF intensity distributions.

An exactly similar, but opposite, trend of the XRF intensity variation is observed in Fig. 4a for WL_α transition of WO_3 at $2\theta = 43°$ in these samples. We also studied the powders pelletized at different pressures of 5–20 tons cm^{-2}. The results are included in Figs 3 (b and c) and 4 (b, c and d). We observed a very systematic variation in intensity from samples A to E in both SiK_α and WL_α transitions. Effectively big particles of 106 μm in sample A had now automatically

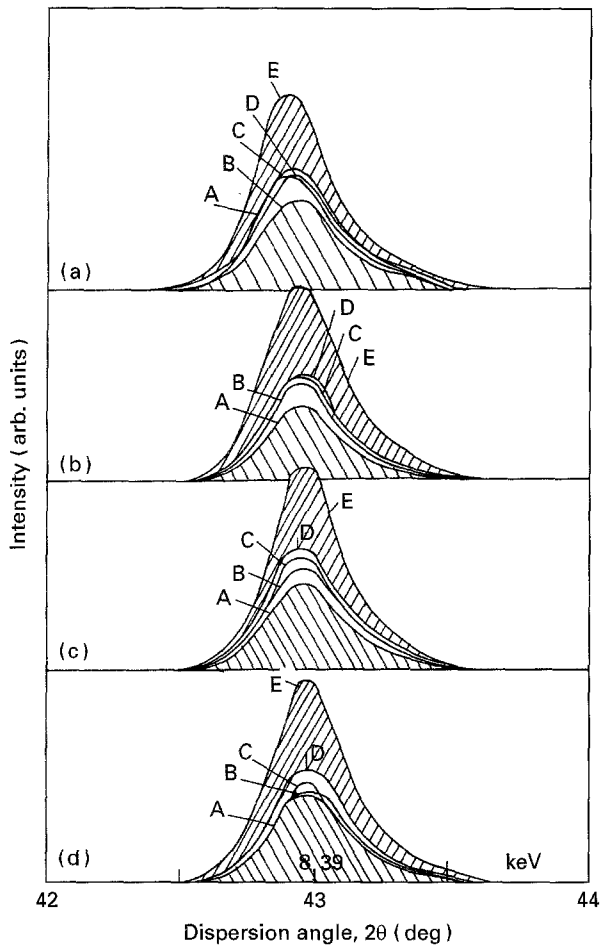

Figure 4 XRF of WO_3 in the wolframite ore of Fig. 3; (a) as-received powders and those pelletized at (b) 5, (c) 10 and (d) 20 tons cm^{-2} applied pressures.

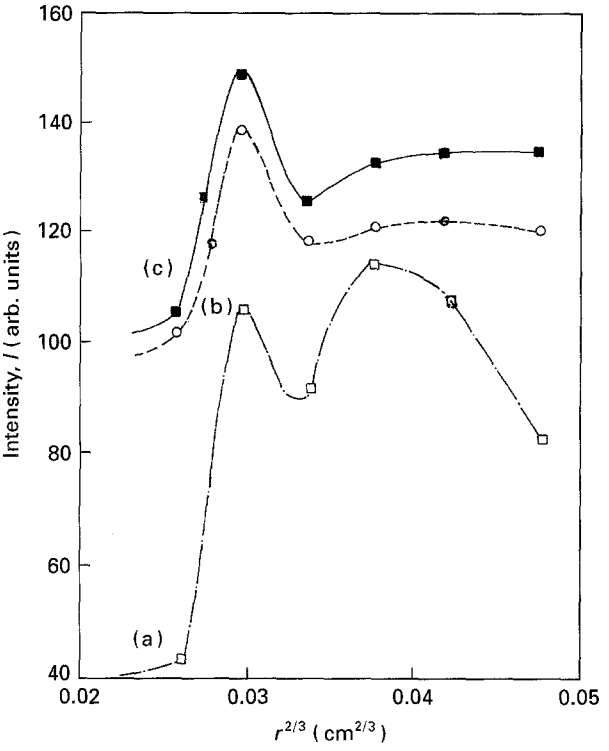

Figure 5 I versus $r^{2/3}$ plot for the SiO_2 fluorescence in the wolframite ore; (a) as-received powders, and those pelletized at (b) 5 and (c) 10 tons cm^{-2} applied pressures.

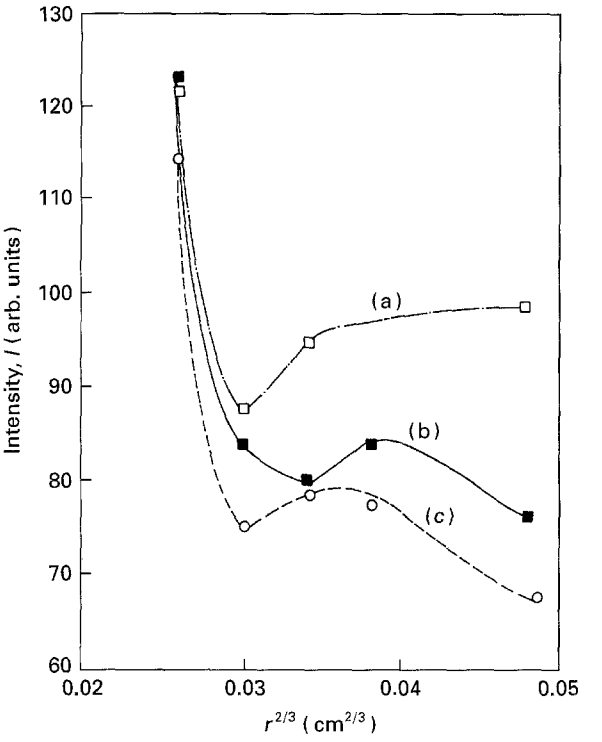

Figure 6 I versus $r^{2/3}$ plot for WO_3 fluorescence in the wolframite ore; (a) as-received powders, and those pelletized at (b) 5 and (c) 10 tons cm^{-2} applied pressures.

fragmented into reasonably smaller pieces subject to the pressure applied to pelletize them and therefore obeyed the trend shown by the other samples, having relatively small-sized particels.

The integrated intensity I in the separated particles of constituent phases of the wolframite ore is a function of the pressure applied to compress them as pellets. A most realistic relation between I and the particle size r is demonstrated by I versus $r^{2/3}$ plots as shown in Figs 5 and 6 for SiK_α and WL_α transitions of SiO_2 and WO_3 in the ore. The I versus $r^{2/3}$ plot reveals a rapid increase of I value for SiK_α signal at the expense of that in the WL_α signal over 45–60 μm sized particles, showing their optimum I values at apparently the same critical size (r^*) ~50 μm of the particles. This observation supports the hypothesis of Madlem [10] that the optimum I value occurs over a particular particle size according to the atomic numbers of the constituent elements. Thus the SiO_2, with significantly lower molecular weight of 60.1 amu compared to 231.9 amu for WO_3, exhibits the precise and optimum fluorescence on considerably bigger particles of 45–60 μm when compared to those (roughly 35 μm) for WO_3. Unfortunately, we did not cover the measurements of XRF over a sufficiently wide range of particle sizes of WO_3, but the I versus $r^{2/3}$ plot (Fig. 6) clearly indicates that it exhibits a maximum intensity on particle sizes very close to 35 μm. Actually, the production of such fine powders of WO_3, which is a characteristically very hard material, is not possible by mechanical attrition without destroying its crystalline structure.

Moreover, the mechanism by which the XRF intensity of the SiK_α signal in SiO_2 varies with WO_3 additions and vice versa is not clear. In this case, the sum of total intensities in the two SiK_α and WL_α signals may

be a more reliable parameter for accurate analysis of these ores. The total intensity I_t in the present example has been found overall to be rapidly enhanced as a function of the pressure (P) applied to compress the powders into their pellets. For the reasonably separated and small sized particles of SiO_2 and WO_3, the value of I_t becomes almost constant in the pellets compressed at about 5 ton cm^{-2} pressures and thus provides a reproducible experimental value in Fig. 7a. The I_t does not vary regularly with P in the eventual case of big particles, as shown in curves (b) and (c) in Fig. 7, because the particles of individual phases are not separated. As such they firmly stick together but break-up into individual components and set-up irregularly, subject to the pressure applied to compress them to form the pellets, to disallow uniform exposure to the incident X-ray beam.

In the most general case, the variation of the integrated intensity I with particle size r can be modelled using an empirical relation

$$I = I_0\left[1 + \left(\frac{\varepsilon}{r^n}\right)F\right] \quad (1)$$

where I_0 is the intrinsic value of I which should be constant for an assembly of noninteracting particles, ε is the dynamic distortion in the crystal lattice or local structures of the associated species, F is geometrical factor, which is governed by morphology of the particles, and n is an exponent.

In the above relation, the constant n describes the contribution of effective size of the particles to fluoresce with the X-ray radiation used to excite the specimen in order to monitor the XRF spectrum. We tried several $I = f(r^n)$ functions and found that a purely empirical value of $n = 2/3$ yields the best representation of the data. The plot between I and $r^{2/3}$ (in Fig. 5) exhibits a peak at $r^* \sim 50$ μm for SiK_α signal of SiO_2 independent of the pressure P. A similar trend is maintained in the WL_α signal of WO_3 in Fig. 6, except the value of I appeared to be minimum for nearly the same $r^* \sim 50$ μm values.

The ores with two or more crystalline or amorphous phases are essentially composite materials whose optical properties are often described by the effective-medium theory, in which macroscopic electromagnetic interactions between two phases are taken into account [11–13]. Assuming that the small spheres of one component are embedded in the matrix of the other component, it predicts an average dielectric function [11],

$$\varepsilon_{av}(\omega) = \varepsilon_m(\omega)\left[1 + 3f\left\{\frac{\varepsilon(\omega) - \varepsilon_m(\omega)}{\varepsilon(\omega)\ (1-f) + \varepsilon_m(\omega)\ (2+f)}\right\}\right] \quad (2)$$

where f is the volume fraction of the secondary phase, of the dielectric function $\varepsilon_m(\omega)$, and $\varepsilon(\omega)$ is the dielectric function of main phase (here SiO_2). This formula is restricted to small f, as in the present example, because it treats two components of the composite materials in an asymmetric manner.

Fujii *et al.* [14] studied infrared absorption of SiO_2 with the additions of Ge microcrystals and observed very similar results to those we observed by XRF for the wolframite ores. They found the frequency ω_{LO}, in LO (longitudinal optical) mode of vibration of SiO_2 at 1240 cm^{-1}, to be almost independent of f but the frequency ω_{TO}, in TO (transverse optical) mode at 1080 cm^{-1}, shifted by about 1% to higher frequencies as f increased from 0 to 0.20. Moreover, the intensities and half-bandwidths in both LO and TO bands were found to be rather more sensitively varied, by a factor as large as 2, with a function of f.

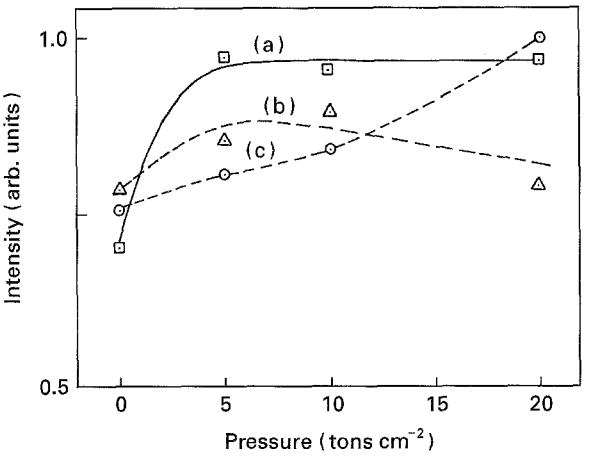

Figure 7 Variation of total XRF intensity (normalized to unity) in SiK_α and WL_α signals in the wolframite ore (powders) as a function of pressure applied to compress them into pellet forms; particle size (a) 44, (b) 63 and (c) 106 μm.

The observed variations in LO and TO frequencies have been successfully reproduced (for example, see Fig. 4 in [14]) using the $\varepsilon_m(\omega)$ values of SiO_2 and Ge microcrystals together with their relative fractions f in Relation (2). A phenomenologically similar relation, which, of course, we have proposed in Equation (1), applies to XRF of the composite materials. Here, it must be mentioned that in the vibrational as well as the electronic (including the XRF) transitions, the dynamic distortion parameter ε, proposed in relation (1), is a particularly important parameter to model the intensity and bandwidth of the involved signal. We are continuing the work to resolve this problem and the results will be communicated separately.

4. Conclusions

We observed that the intensity of X-ray fluorescence of SiO_2 varies with a function of particle size (over 30–110 μm) or its volume fraction in presence of a secondary phase of WO_3 in the binary mixture or in a wolframite ore having these two major phases. The most drastic and interesting spectral change was the increase of SiO_2 fluorescence (at 1.741 keV transition energy) at the expense of WO_3 fluorescence at 8.39 keV over 45–60 μm sized particles. According to the effective medium theory, the macroscopic electromagnetic interactions between the individual particles of two phases dispersed homogeneously one over the other play a dominant role in determining the X-ray fluorescence. The novel results we reported here are very helpful for understanding the nonlinear response of small-sized particles, of the order of several

micrometers to a few nanometers, of minerals, ores or similar other materials to their X-ray fluorescence, which is a nondestructive technique and conveniently applied to rapidly analyse elemental compositions of desired specimens.

Acknowledgements

The authors are thankful to Professor P. Ramachandrarao, Director, National Metallurgical Laboratory, Jamshedpur, for fruitful discussions, encouragement and permission to publish this paper.

References

1. P. F. BERRY, T. FURUTA and J. R. RODES, *Adv. X-ray Anal.* **12** (1969) 612.
2. F. CLAISSE and C. SAMSON, *ibid.* **5** (1961) 335.
3. F. BERNSTEIN, *ibid.* **5** (1961) 486.
4. S. RAM, *Phys. Rev.* (*B*) **51** (1995) 6280.
5. *Idem, J. Mater. Sci.* **25** (1990) 2465.
6. S. RAM, K. RAM and B. S. SHUKLA, *ibid.* **27** (1992) 511.
7. J. P. RINO, I. EBBSJO, R. K. KALIA, A. NAKANO and P. VASHISHTA, *Phys. Rev.* (*B*) **47** (1993) 3053.
8. S. C. SRIVASTAVA, *J. Mines, Metals Fuels* **26** (1978) 413.
9. S. C. SRIVASTAVA, RAJEEV and M. K. GHOSH, *ibid.* **28** (1980) 22.
10. K.W. MADLEM, *Adv. X-ray Anal.* **9** (1965) 441.
11. L. GENZELI and T. P. MARTIN, *Phys. Stat. Solidi* (*B*) **51** (1972) 91.
12. T. WON NOH, Y. SONG, S. LEE, J. R. GRAINS, H. D. PARK and E. R. KREIDLER, *Phys. Rev.* (*B*) **33** (1986) 3793.
13. M. F. McMILLAN and R. P. DEVATY, *ibid.* **43** (1991) 13838.
14. M. FUJII, M. WADA, S. HAYASHI and K. YAMAMOTO, *ibid.* **46** (1992) 15930.

Received 23 August 1994
and accepted 28 April 1995